Biochemical and Biophysical Research Communications 425 (2012) 938–943

Contents lists available at SciVerse ScienceDirect

Biochemical and Biophysical Research Communications

journal homepage: www.elsevier.com/locate/ybbrc

1-(2,6-Dibenzyloxybenzoyl)-3-(9H-fluoren-9-yl)-urea: A novel cyclophilin A allosteric activator

Maosheng Lv [a,1], Ting Shi [b,1], Xiaona Mao [a,1], Xi Li [a], Yingyi Chen [b], Jin Zhu [a,*], Shuaishuai Ni [a], Xu Shen [a,c], Hualiang Jiang [a,c], Jian Li [a], Jian Zhang [b,*], Jin Huang [a,*]

[a] Shanghai Key Laboratory of New Drug Design, School of Pharmacy, East China University of Science and Technology, 130 Meilong Road, Shanghai 200237, China
[b] Department of Pathophysiology, Key Laboratory of Cell Differentiation and Apoptosis of Chinese Ministry of Education, Shanghai JiaoTong University, School of Medicine, 227 South Chongqing Road, Shanghai 200025, China
[c] Drug Discovery and Design Center, Shanghai Institute of Materia Medica, Chinese Academy of Sciences, 555 Zu Chong Zhi Road, Shanghai 201203, China

ARTICLE INFO

Article history:
Received 13 July 2012
Available online 11 August 2012

Keywords:
CypA
PPIase activity
Allosteric activator
Chemical tool

ABSTRACT

Cyclophilin A (CypA) plays an important role in many physiology processes and its overexpression has been involved in many diseases including immune disease, viral infection, neuro-degenerative disease, and cancer. However, the actual role of CypA in the diseases is still far from clear, and a complete understanding of CypA is necessary in order to direct more specific and effective therapeutic strategies. Based on the screening of our in-house library through the isomer-specific proteolysis method, we find a CypA activator (1-(2,6-Dibenzyloxybenzoyl)-3-(9H-fluoren-9-yl)-urea), compound **1a**, which can increase CypA's PPIase activity and give allosteric behavior. The binding affinity of compound **1a** to CypA has been confirmed by Fortebio's Octet RED system and the increased phosphorylation of ERK in H446 cells is observed by treatment with both compound **1a** and CsA. In order to further evaluate the binding mode between the activator and CypA, the allosteric binding site and allosteric mechanism of CypA are investigated by molecular dynamics (MD) simulations in combination with mutagenesis experiments. The results show that the allosteric binding site of CypA is 7 Å away from its catalytic site and is composed of Cys52, His70, His54, Lys151, Thr152 and Lys155. Compound **1a** binds to the allosteric site of CypA, stabilizing the active conformation of catalytic residues, and finally promotes the catalytic efficiency of CypA. We believe our finding of the CypA allosteric activator will be used as an effective chemical tool for further studies of CypA mechanisms in diseases.

1. Introduction

Cyclophilin A (CypA), a member of the ubiquitous cyclophilin family, is initially purified from bovine thymocytes [1]. CypA catalyzes the *cis–trans* isomerization of peptidyl–prolyl bonds in peptides and proteins [2,3], and plays an important role in many physiological processes including protein folding, transportation, assembly, immune modulation and cell signaling [4–7]. It has been reported that the overexpression of CypA is associated with many diseases such as immune disease, viral infection, neuro-degenerative disease, and cancer [8–13].

CsA (Cyclosporin A) is an undecapeptide produced by a variety of fungi imperfecti, notably *Tolypocladium inflatum*, and can specifically bind to the catalytic site of CypA with high affinity, which is now widely used as immunosuppressant for human organ and tissue transplantation [14]. However, the side effects in clinical CsA therapy are thought to induce cancers [15], such as skin cancer, lymphoma and Kaposi sarcoma [16]. Therefore, the mechanism of CypA is still far from clear in physiological and pathological conditions and a more complete understanding of the biological profile induced by CypA needs to be resolved. In recent years, chemical probes are widely utilized to investigate the underlying mechanism in the biological network and much impressive progress in this field has been made in a remarkably short time [17–19]. Considering the advantages in the investigation of biological profiles achieved through chemical tools, the finding of this CypA probe may make an important effect on unraveling the secrets of CypA transduction. Herein, we report a small molecular compound **1a** (1-(2,6-Dibenzyloxybenzoyl)-3-(9H-fluoren -9-yl)-urea) as an allosteric activator of human CypA. Compound **1a** was screened by the PPIase activity and confirmed through binding affinity assay, and its effect on ERK (extracellular regulated protein kinases) phosphorylation was tested at the cell level. The allosteric binding site and the allosteric mechanism of compound **1a** were also presented by mutagenesis experiments and molecular dynamics

* Corresponding authors. Fax: +86 2164253681.
E-mail addresses: jinz@ecust.edu.cn (J. Zhu), jian.zhang@sjtu.edu.cn (J. Zhang), huangjin@ecust.edu.cn (J. Huang).
[1] These authors contributed equally to this work.

0006-291X/$ - see front matter © 2012 Elsevier Inc. All rights reserved.
http://dx.doi.org/10.1016/j.bbrc.2012.08.014

(MD) simulations. The above studies suggest that compound **1a** is an allosteric activator of CypA and could be used as a chemical probe for uncovering mechanisms of CypA in the biological network.

2. Materials and methods

2.1. Protein expression and purification

Expression plasmid pET15b-CypA was a kindly gift from the center of medical laboratory sciences, Nanjing PLA Hospital. Wild type or mutant CypA was expressed in *Escherichia coli* BL21 cells and purified as described previously [19].

2.2. PPIase activity assay

PPIase activity assays of human wild-type or mutant CypA were performed as our previously procedures with a little modification [19]. Briefly, 20 μl CypA stock solution (500 nM, in 20 mM Tris–HCl, 50 mM NaCl, pH 7.8) was diluted in 460 μl assay buffer (20 mM Tris–HCl, 50 mM NaCl, pH 7.8) at 4 °C, then 10 μl of α-chymotrypsin (20 mg/mL in 1 mM HCl) was added, and the reaction was initiated by adding 10 μl of substrate (AAPF, 2 mg/mL in 500 mM LiCl in THF). The absorption at 384 nm was measured immediately when the reaction was initiated. To determine the activation activity, compound **1a** with various concentrations was incubated with the CypA solution for 2 h at 4 °C, and then the PPIase activity assay was carried out.

2.3. The binding affinity assay of *1a* and CypA by Fortebio's Octet system

Before the experiment, 50 μM purified CypA was dissolved in dialysis buffer (40 mM HEPES, pH 7.8) and biotinylated by adding equivalent biotin for 30 min. Then the unconjugated biotin was removed by using PD-10 desalting column (Catalog number 17-0851-01, GE Healthcare). The sensors (Super Streptavidin, SSA) were pre-wet in dialysis buffer for 15 min prior to use. For binding affinity assay, the sensors were loaded with biotinylated CypA for 15 min, then quenched in 10 μM biocytin for 1 min. Compound **1a** was prepared in a serial dilution (25, 50 and 100 μM), and the concretely empirical procedure installation was shown as Supporting information, Table S1. The sensors without loading biotinylated CypA were used as a control to correct for baseline drift. The whole process of experiment was carried out at room temperature.

2.4. Site-directed mutagenesis of CypA

All the 27 mutants were generated from the expression plasmid pET15b-CypA, according to QuickChange Site-Directed Mutagenesis Kit manual. Forward primers for generation of each mutant were listed in Supporting information, Table S2. All the mutations were verified by sequencing at Invitrogen.

2.5. Cell culture

H446 cells were cultured in RPMI-1640 supplemented with 10% FBS, and maintained at 37 °C in 5% CO_2 atmosphere.

2.6. Western bolt

H446 Cells were lysed by adding lysis buffer (20 mM Tris, 150 mM NaCl, 1% Triton X-100, pH 7.5), supplemented with protease inhibitor cocktail and phosphotase inhibitor cocktail, and then the supernatant was collected. Proteins were separated by SDS–PAGE, and were transferred to polyvinyldifluoride membrane by electroblotting. Anti-phospho-ERK (T202/Y204) and ERK (D196) antibodies (Bioworld) were used, and the immunodetection was performed by standard techniques using chemiluminescence.

2.7. Docking simulation between compound *1a* and CypA

The X-ray crystal structure of CypA (PDB entry: 1M9C, 2.0 Å resolution) [20] was extracted as docking receptor template, and then the GLIDE software [21,22] was used to probe location of compound **1a** in the CypA. All the default parameters were used during the docking after the protein structures were prepared in "Protein Preparation Wizard" and SK compounds were prepared in "LigPrep". The binding pocket in the docking was defined to the whole CypA. Multiple docking runs were iteratively performed till no remarkable difference (RMSD > 2.0) in new conformations has been generated. Then, a conformational clustering script encoded in the Autodock [23,24] was used to classify docking poses and the second binding site topologically distinct from orthosteric site was selected according to main cluster of conformations on the non-orthosteric site of CypA.

2.8. Molecular dynamics (MD) simulations

The structures of CypA and CypA-compound **1a** were taken as the starting points for molecular dynamics simulations. Each MD simulation was carried out using the AMBER suite of programs (version 8.0) with the parm99 force field [25]. The charges of the atoms of compound **1a** were calculated by using the RESP method [26] encoded in the AMBER at the level of RHF/6-31G*. Covalent and nonbonded parameters for the activator atoms were assigned by analogy or through interpolation from those already present in the AMBER force field [25]. Each system was prepared by using the xLeap module in AMBER, in which protons were added to the structure. All ionizable side-chains were maintained in their standard protonation states at pH 7.4. The proteins were solvated in cubic box of TIP3P water molecules, with a water thickness extending at least 10 Å apart from the protein surface. To avoid the instability that might occur during the MD simulations, the solvated system was subjected to minimization for 5000 cycles with protein restrained and followed by another 5000 cycles with the whole system relaxed. Then, the system was gradually heated from 0 to 300 K during the first 60 ps by three intervals, followed by equilibrium for 80 ps under constant volume and temperature (NVT) condition. Afterwards, the system was switched to constant pressure and temperature (NPT) condition and equilibrated for 100 ps to adjust the system to a correct density. Finally, the production simulations were carried out in the absence of any restraint under NPT condition and two 4-ns MD simulations were then conducted on the CypA and CypA-compound **1a** to probe the function of compound **1a**. This protocol was applied to all of the simulation systems.

All the MD simulations were performed using the parallel version of PMEMD in AMBER suit. The particle mesh Ewald method was employed to calculate the long-range electrostatic interactions, whereas the lengths of the bonds involving hydrogen atoms were fixed with the SHAKE algorithm [27,28]. During the simulations, the integration time step of 2 fs was adopted and structural snapshots were flushed every 500 steps (1 ps). The non-bonded cutoff was set to 10.0 Å, and the non-bonded pair list was updated every 25 steps. Each production simulation was coupled to a 300 K thermal bath at 1.0 atm pressure by applying the Berendsen algorithm [29]. The temperature and pressure coupling constants were set to 2.0 and 1.0 ps, respectively.

2.9. Preparation of compound **1a**

The synthesis details of compound **1a** were described in the Supporting information.

3. Results and discussion

3.1. Compound **1a** can bind to CypA and increase the PPIase activity of CypA

By screening an in-house library of ~500 compounds against human wild type (wt) CypA protein, we found a compound **1a** that could improve catalytic activity on CypA (Fig. 1). Synthetic procedures and structural characterizations of compound **1a** were described in Supporting information. PPIase activities of CypA were determined by a spectrophotometric method based on isomer-specific proteolysis. First, CypA was incubated with compound **1a** (10 μM) for 2 h, the catalytic efficiency of CypA (PPIase) was observed to increase about 54% (Fig. 1A). Then, compound **1a** (10 μM), CsA (10 μM) and CypA were incubated for 2 h, lead the catalytic efficiency of CypA to increase around 51% (Fig. 1B). Similar result with almost 53% increase of CypA PPIase was also found when compound **1a** (10 μM) was incubated with CypA for 1 h followed by the treatment with CsA (10 μM) for one more hour (Fig. 1C).

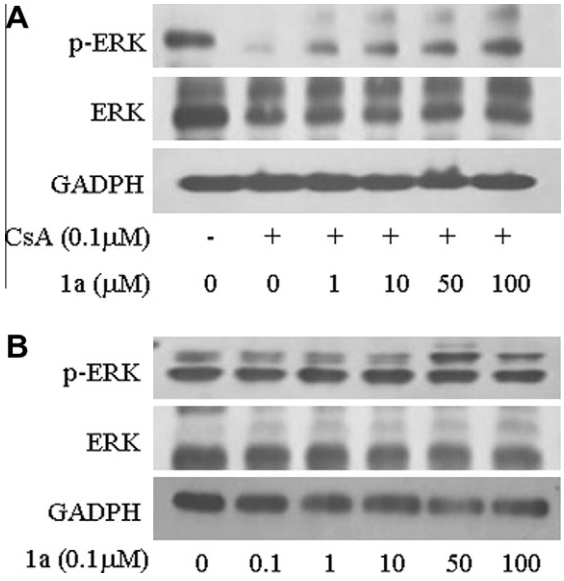

Fig. 2. ERK phosphorylation level in H446 cells treated with different concentrations of compound **1a**. (A): H446 cells were exposed to CsA (0.1 μM) at increasing concentrations (0–100 μM) of compound **1a** for 48 h; (B): H446 cells were exposed to different concentration (0–100 μM) of compound **1a** for 48 h.

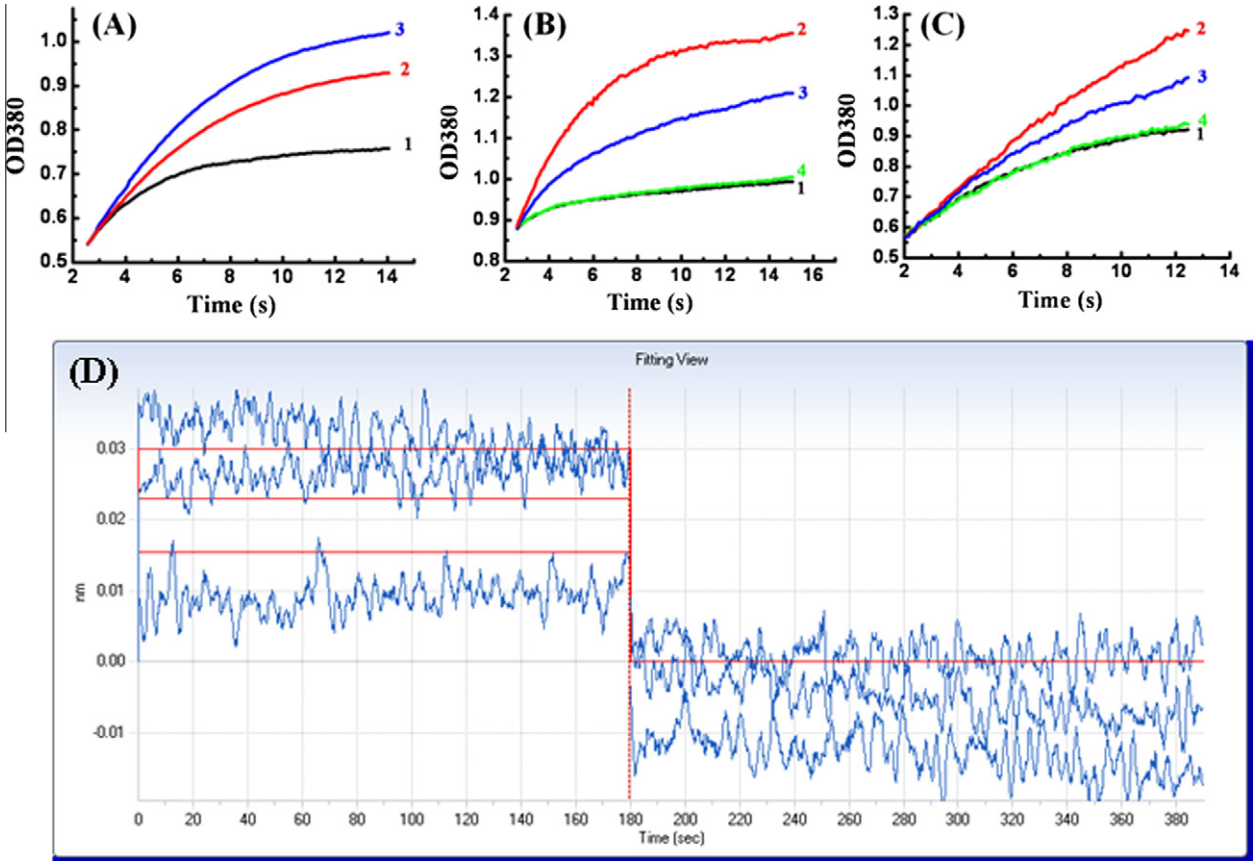

Fig. 1. The allosteric efficiency of compound **1a** to the PPIase activity of CypA and the binding affinity of compound **1a** to CypA. (A) Curve 1, control, without CypA; Curve 2, the PPIase activity of CypA; Curve 3, the PPIase activity of CypA which incubated with 10 μM compound **1a** for 2 h. (B) Curve 1, control, without CypA; Curve 2, the PPIase activity of CypA; Curve 3, the PPIase activity of CypA which incubated with both 10 μM CsA and 10 μM compound **1a** for 2 h; Curve 4, the PPIase activity of CypA which incubated with 10 μM CsA for 2 h. (C) Curve 1, control, without CypA; Curve 2, the PPIase activity of CypA; Curve 3, the PPIase activity of CypA which incubated with 10 μM compound **1a** for 1 h, then add 10 μM CsA and incubated for more 1 h; Curve 4, the PPIase activity of CypA which incubated with 10 μM CsA for 2 h. (D) The binding affinity of compound **1a** to CypA. Left part represents the dissociation curve of compound **1a** and CypA; right part shows the association curve, the concentrations of compound **1a** used for the test were 25, 50 and 100 μM, respectively.

Table 1
The catalytic efficiency of compound **1a** to different CypA mutations.

Residue num	Mutation	Position	Catalytic efficiency
None (wide type)			43.7%
Cys52	Phe	Binding site	0%
Cys52	Ser	Binding site	6%
Cys52	Leu	Binding site	19.8%
Cys52	Ala	Binding site	39.2%
His54	Trp	Binding site	34.3%
Arg55	Ala	Binding site	24.8%
Arg55	Trp	Binding site	22.6%
His70	Arg	Binding site	2.3%
His70	Trp	Binding site	37.8%
Lys151	Ala	Binding site	38.0%
Thr152	Phe	Binding site	19.5%
Thr152	Trp	Binding site	17.5%
Thr152	Ala	Binding site	49.5%
Lys155	Ala	Binding site	25.8%
Glu23	Ala	Periphery	37.9%
Phe46	Ala	Periphery	45.2%

To investigate the action of compound **1a**, the binding affinity of compound **1a** to CypA *in vitro* was tested by Fortebio's Octet RED System (Supporting information, Table S1), and the result showed the dissociation constant K_D of $4.50 \pm 0.03 \times 10^{-5}$ M (Fig. 1D).

3.2. The activation effect of Compound *1a* in cells

It was reported that CypA could bind and activate the cell surface receptor CD147, leading to the activation of the ERK signaling pathway, and that CsA could block this effect of CypA [30]. In order to determine whether the activation effect of compound **1a** existed at the cell level, H446 cells were exposed to different concentrations of compound **1a** in the absence or presence of CsA and the effect of compound **1a** on ERK phosphorylation was evaluated. Western blot analysis showed that treatment with compound **1a** for 48 h had little effect on the phosphorylation of ERK in cells. But in the treatment combined with CsA, compound **1a** could improve the phosphorylation of ERK in a dose-dependent manner (Fig. 2). All the above observations indicated that compound **1a** was not only a low-affinity ligand to CypA, but also an allosteric activator of CypA.

3.3. The molecular mechanism between compound *1a* and CypA

To research the molecular mechanism of compound **1a** behind allosteric activation, a hybrid method integrating docking simulation with mutagenesis validation was used to identify the binding site of compound **1a** to CypA. The docking analysis showed that residues around Cys52 might be the binding site of compound **1a**. Based on the results, several amino acid residues, which were thought to play a vital role in the binding mode of compound **1a**, were further tested by site-directed mutagenesis experiments. The catalytic efficiency of compound **1a** on 27 CypA mutants was determined (Table 1). Compared with wt-CypA, we found the mutations of Cys52, Arg55, His70, Thr152 and Lys155 significantly decreased the catalytic efficiency of compound **1a** (Table 1), indicating their involvement in the allosteric pocket. It should be

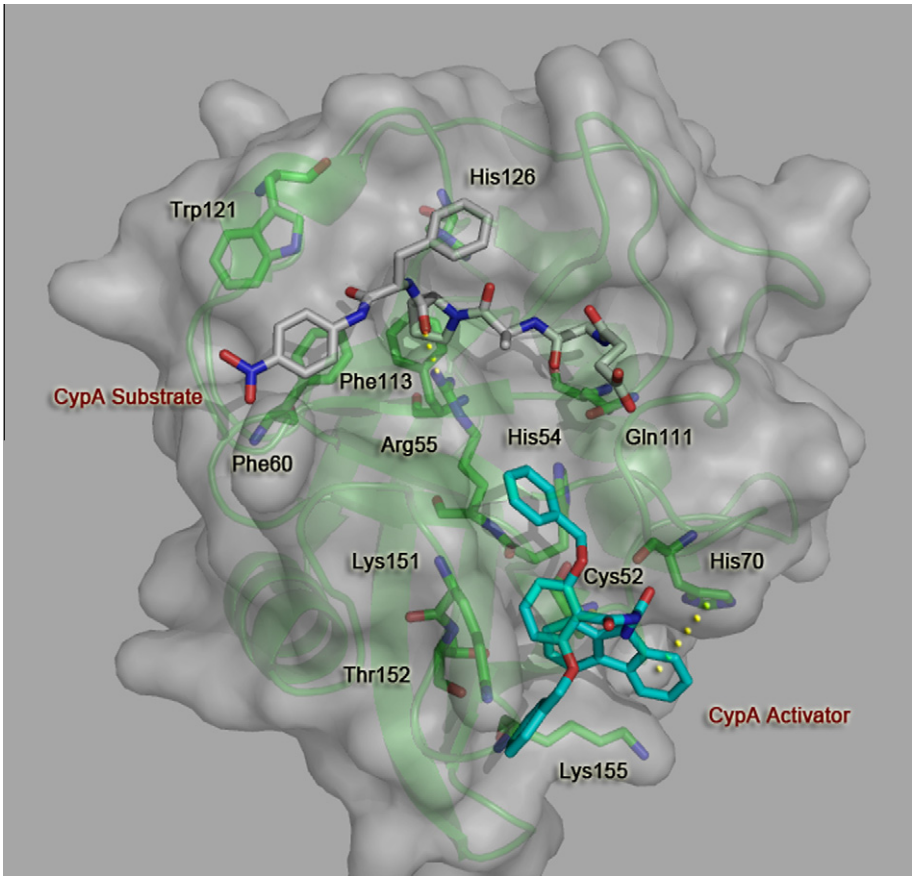

Fig. 3. The allosteric binding model of compound **1a** to CypA with the presence of substrate. CypA predicted docking model revealed both substrate site and allosteric site of CypA. For protein, carbon atoms of the human CypA were shown in green, oxygen atoms in red, and nitrogen atoms in blue. Side chains of crucial residues in the allosteric binding site are shown as stick and labeled. For ligands, carbon atoms of substrate are colored in white and those of allosteric activator are colored in cyan. Hydrogen bonds between ligands and protein were depicted in dotted line in yellow. (For interpretation of the references to colour in this figure legend, the reader is referred to the web version of this article.)

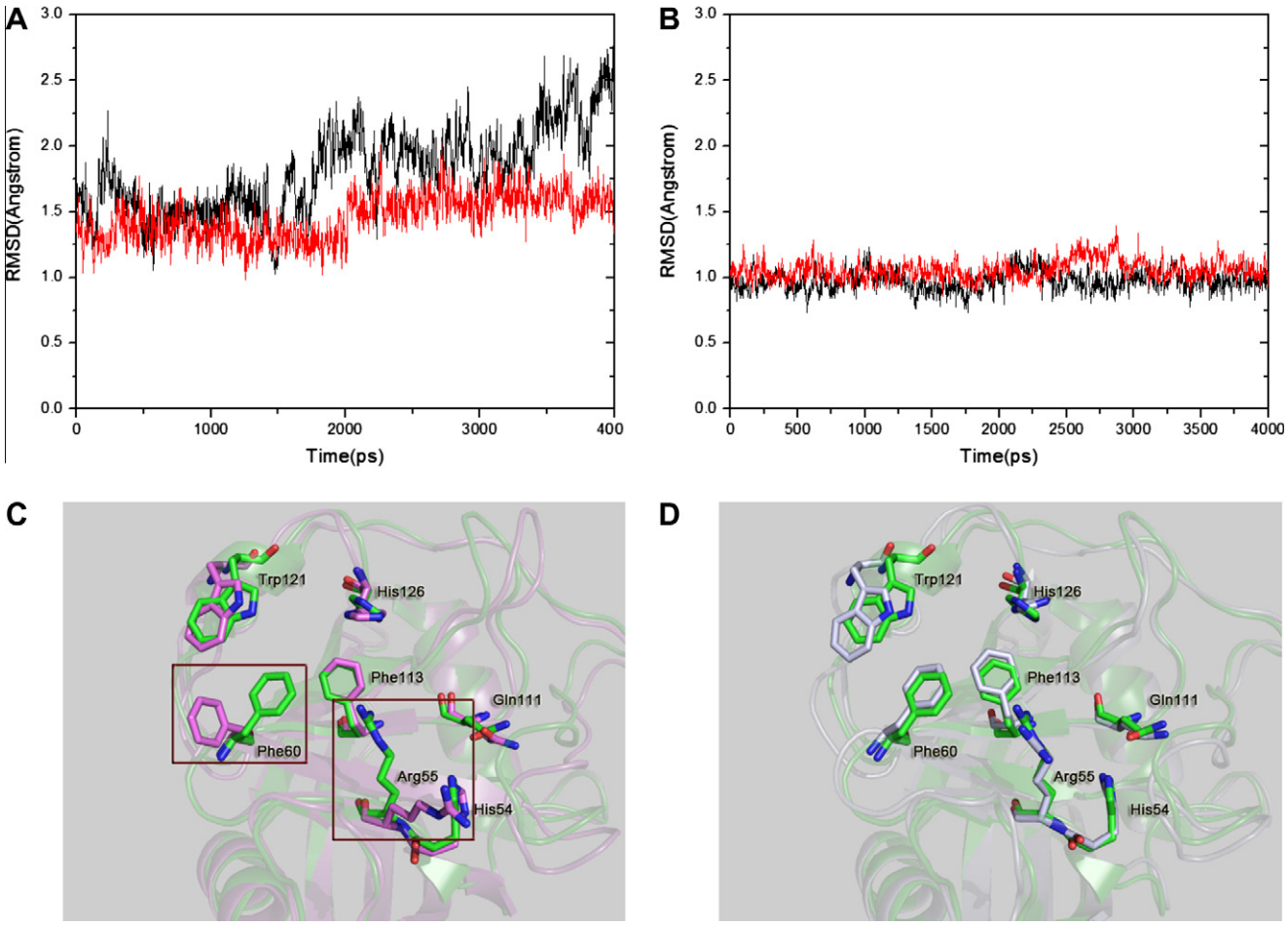

Fig. 4. The allosteric mechanism of compound **1a** in CypA from MD simulations. The stability of key residues in the active pocket (A) and the whole protein (B) in 4-ns simulations of CypA, in which the system of CypA with compound **1a** is colored in red and CypA without compound **1a** is colored in black; (C) The view of substrate binding pocket from the simulation of CypA without compound **1a**, carbon atoms in the crystal CypA as superimposed reference are green and in the final snapshot from the simulation are pink; (D) The view of substrate binding pocket from the simulation of CypA with compound **1a**, carbon atoms in crystal CypA as superimposed reference are green and in the final snapshot from the simulation are white. All side chains of crucial residues in the binding site of substrate are shown as stick and labeled in (C) and (D). (For interpretation of the references to colour in this figure legend, the reader is referred to the web version of this article.)

pointed out that the CypA PPIase activity was totally lost when Cys52 was mutated to Phe, implying that Cys52 might be a crucial residue for compound **1a** to bind CypA. Furthermore, His70 was believed as an important residue for the binding of compound **1a** to CypA, as the π-π interaction may exist between the imidazole ring of histidine and 9*H*-fluorene group of compound **1a**. This finding was verified by the lost catalytic efficiency of the H70 W mutant (Table 1). The binding model of compound **1a** to CypA with the presence of substrate was shown in Fig. 3. Our findings located the allosteric site of compound **1a** and demonstrated the function of key residues.

In order to fully understand the allosteric mechanism of the system at the atomic detail, two models of CypA with (model I, red color) and without (model II, black color) compound **1a** were respectively designed for molecular dynamics (MD) simulations, and 4-ns simulations were performed to explore both the stability of some key residues in the active pocket (Fig. 4A) and the conformational changes of the whole system (Fig. 4B). Seven key residues, including His54, Arg55, Phe60, Gln111, Phe113, Trp121 and His126, were involved in the catalytic activity of CypA as shown in Fig. 3. RMSD of the key residues in the simulations was found to be more stable when compound **1a** bound to the allosteric site (Fig. 4A), although the stability of the whole system did not show an obvious difference between model I and model II (Fig. 4B). Furthermore, the final snapshots from the simulations were extracted and superimposed into the crystal of CypA, and the seven key residues were carefully evaluated in Fig. 4C and 4D. When compound **1a** was absent (Fig. 4C, pink color), Arg55 and Phe60 moved away from the catalytic site, made the catalytic pocket enlarged, and the substrate to escape easily, resulting in the reduction of the catalytic efficiency. Conversely, the residues kept their active orientation in the catalytic pocket when compound **1a** existed. This result indicated that compound **1a**, as a CypA activator, could maintain the catalytic pocket in a stable and efficient conformation and furthermore accelerate the catalysis of substrate, which had been partly proven by Donald's report [31] where Arg55 acted as an anchor for the substrate in the binding site. We believe this CypA activator and its allosteric mechanism might have important implications for the design of CypA allosteric activators and compound **1a** could be used as a probe for further studies *in vivo*.

Acknowledgment

We gratefully acknowledge the financial supports from the National Natural Science Foundation of China (81102420, 21002028, and 21002062), National S&T Major Project, China (Grant 2011ZX09102-005-02), the Program for Professor of Special

Appointment (Eastern Scholar) at Shanghai Institutions of Higher Learning, Shanghai PuJiang Program (10PJ406800), the Shanghai Committee of Science and Technology (Grant 11DZ2260600) and the Fundamental Research Funds for the Central Universities.

Appendix A. Supplementary data

Supplementary data associated with this article can be found, in the online version, at http://dx.doi.org/10.1016/j.bbrc.2012.08.014.

References

[1] R.E. Handschumacher, M.W. Harding, J. Rice, R.J. Drugge, D.W. Speicher, Cyclophilin: a specific cytosolic binding protein for cyclosporin A, Science 226 (1984) 544–547.
[2] G. Fischer, T. Tradler, T. Zarnt, The mode of action of peptidyl prolyl cis/trans isomerases in vivo: binding vs. catalysis, FEBS Lett. 426 (1998) 17–20.
[3] G. Fischer, H. Bang, The refolding of urea-denatured ribonuclease A is catalyzed by peptidyl–prolyl cis–trans isomerase, Biochim. Biophys. Acta, Protein Struct. Mol. Enzymol. 828 (1985) 39–42.
[4] J. Colgan, M. Asmal, M. Neagu, B. Yu, J. Schneidkraut, Y. Lee, E. Sokolskaja, A. Andreotti, J. Luban, Cyclophilin A regulates tcr signal strength in CD4+ T Cells via a proline-directed conformational switch in Itk, Immunity 21 (2004) 189–201.
[5] A. Galat, Peptidylproline cis-trans-isomerases: immunophilins, Eur. J. Biochem. 216 (1993) 689–707.
[6] J.L. Kofron, P. Kuzmic, V. Kishore, E. Colon-Bonilla, D.H. Rich, Determination of kinetic constants for peptidyl prolyl cis-trans isomerases by an improved spectrophotometric assay, Biochemistry 30 (1991) 6127–6134.
[7] K. Arora, W.M. Gwinn, M.A. Bower, A. Watson, I. Okwumabua, H.R. MacDonald, M.I. Bukrinsky, S.L. Constant, Extracellular cyclophilins contribute to the regulation of inflammatory responses, J. Immunol. 175 (2005) 517–522.
[8] M. Harigai, M. Hara, N. Takahashi, A. Kitani, T. Hirose, K. Suzuki, M. Kawakami, T. Hidaka, Y. Kawaguchi, T. Ishizuka, Presence of autoantibodies to peptidyl-prolyl cis-trans isomerase (cyclosporin A-binding protein) in systemic lupus erythematosus, Clin. Immunol. Immunopathol. 63 (1992) 58–65.
[9] J. Luban, K.L. Bossolt, E.K. Franke, G.V. Kalpana, S.P. Goff, Human immunodeficiency virus type 1 Gag protein binds to cyclophilins A and B, Cell 73 (1993) 1067.
[10] E.K. Franke, H.E.H. Yuan, J. Luban, Specific incorporation of cyclophilin A into HIV-1 virions, Nature 372 (1994) 359–362.
[11] K. Goto, K. Watashi, D. Inoue, M. Hijikata, K. Shimotohno, Identification of cellular and viral factors related to anti-hepatitis C virus activity of cyclophilin inhibitor, Cancer Sci. 100 (2009) 1943–1950.
[12] F.M. Göldner, J.W. Patrick, Neuronal localization of the cyclophilin A protein in the adult rat brain, J. Comp. Neurol. 372 (1996) 283–293.
[13] R.W. Georgantas, V. Tanadve, M. Malehorn, S. Heimfeld, C. Chen, L. Carr, F. Martinez-Murillo, G. Riggins, J. Kowalski, C.I. Civin, Microarray and serial analysis of gene expression analyses identify known and novel transcripts overexpressed in hematopoietic stem cells, Cancer Res. 64 (2004) 4434.
[14] F. Borrel, C. Feurer, H. Gubler, H. Staehelin, Biological effects of cyclosporine A: a new antilymphocyte agent, Agents Actions 6 (1976) 468.
[15] N. André, B. Roquelaure, J. Conrath, Molecular effects of cyclosporine and oncogenesis: a new model, Med. Hypotheses 63 (2004) 647–652.
[16] I. Penn, Occurrence of cancers in immunosuppressed organ transplant recipients, Clin. Transplant. (1998) 147.
[17] T. Mori, S. Itami, T. Yanagi, Y. Tatara, M. Takamiya, T. Uchida, Use of a real-time fluorescence monitoring system for high-throughput screening for prolyl isomerase inhibitors, J. Biomol. Screening 14 (2009) 419–424.
[18] S. Daum, M. Schumann, S. Mathea, T. Aumüller, M.A. Balsley, S.L. Constant, B.F. de Lacroix, F. Kruska, M. Braun, C. Schiene-Fischer, Isoform-specific inhibition of cyclophilins, Biochemistry 48 (2009) 6268–6277.
[19] S. Ni, Y. Yuan, J. Huang, X. Mao, M. Lv, J. Zhu, X. Shen, J. Pei, L. Lai, H. Jiang, Discovering potent small molecule inhibitors of cyclophilin A using de novo drug design approach, J. Med. Chem. 52 (2009) 5295–5298.
[20] B.R. Howard, F.F. Vajdos, S. Li, W.I. Sundquist, C.P. Hill, Structural insights into the catalytic mechanism of cyclophilin A, Nat. Struct. Biol. 10 (2003) 475–481.
[21] R.A. Friesner, J.L. Banks, R.B. Murphy, T.A. Halgren, J.J. Klicic, T. Daniel, M.P. Repasky, E.H. Knoll, M. Shelley, J.K. Perry, Glide: a new approach for rapid, accurate docking and scoring. 1. Method and assessment of docking accuracy, J. Med. Chem. 47 (2004) 1739–1749.
[22] T.A. Halgren, R.B. Murphy, R.A. Friesner, H.S. Beard, L.L. Frye, W.T. Pollard, J.L. Banks, Glide: a new approach for rapid, accurate docking and scoring. 2. Enrichment factors in database screening, J. Med. Chem. 47 (2004) 1750–1759.
[23] G.M. Morris, D.S. Goodsell, R.S. Halliday, R. Huey, W.E. Hart, R.K. Belew, A.J. Olson, Automated docking using a Lamarckian genetic algorithm and an empirical binding free energy function, J. Comput. Chem. 19 (1998) 1639–1662.
[24] Z. Huang, L. Zhu, Y. Cao, G. Wu, X. Liu, Y. Chen, Q. Wang, T. Shi, Y. Zhao, Y. Wang, W. Li, Y. Li, H. Chen, G. Chen, J. Zhang, ASD: a comprehensive database of allosteric proteins and modulators, Nucleic Acids Res. 39 (2011) D663–669.
[25] J. Wang, P. Cieplak, P.A. Kollman, How well does a restrained electrostatic potential (RESP) model perform in calculating conformational energies of organic and biological molecules?, J Comput. Chem. 21 (2000) 1049–1074.
[26] C.I. Bayly, P. Cieplak, W. Cornell, P.A. Kollman, A well-behaved electrostatic potential based method using charge restraints for deriving atomic charges: the RESP model, J. Phys. Chem. 97 (1993) 10269–10280.
[27] J.P. Ryckaert, G. Ciccotti, H.J.C. Berendsen, Numerical integration of the cartesian equations of motion of a system with constraints: molecular dynamics of n-alkanes, J. Comput. Phys. 23 (1977) 327–341.
[28] S. Miyamoto, P.A. Kollman, SETTLE: an analytical version of the SHAKE and RATTLE algorithm for rigid water models, J. Comput. Chem. 13 (1992) 952–962.
[29] H.J.C. Berendsen, J.P.M. Postma, W.F. Van Gunsteren, A. DiNola, J. Haak, Molecular dynamics with coupling to an external bath, J. Chem. Phys. 81 (1984) 3684.
[30] S. Boulos, B.P. Meloni, P.G. Arthur, B. Majda, C. Bojarski, N.W. Knuckey, Evidence that intracellular cyclophilin A and cyclophilin A/CD147 receptor-mediated ERK1/2 signalling can protect neurons against in vitro oxidative and ischemic injury, Neurobiol. Dis. 25 (2007) 54–64.
[31] D. Hamelberg, J.A. McCammon, Mechanistic insight into the role of transition-state stabilization in cyclophilin A, J. Am. Chem. Soc. 131 (2008) 147–152.